Wang *et al. Journal of Ovarian Research* (2025) 18:58
https://doi.org/10.1186/s13048-025-01641-2

Journal of Ovarian Research

RESEARCH Open Access

MEOX2 mediates cisplatin resistance in ovarian cancer via E2F target and DNA repair pathways

Fei Wang[1,2,3,4], Hao Zhang[1,2,3], Xiru Liu[1,2,3], Yuanyuan Dou[1,2,3] and Hui Yang[1,2,3*]

Abstract

Ovarian cancer (OV) is a leading cause of cancer-related mortality among women worldwide. Despite the success of platinum-based chemotherapy in treating OV, the emergence of cisplatin resistance has significantly compromised its therapeutic efficacy. Therefore, understanding the mechanisms underlying cisplatin resistance and its molecular regulation is crucial for improving patient outcomes. This study, MEOX2 was identified as a key gene significantly associated with prognosis and cisplatin resistance in OV through bioinformatics analysis. Its expression level and biological functions were validated using online databases, tissue microarrays, and cellular experiments. The results demonstrated that high MEOX2 expression was closely associated with poor survival outcomes in OV patients, while its expression was significantly reduced in cisplatin-resistant cells. Further gene silencing experiments revealed that silencing MEOX2 markedly enhanced cisplatin resistance in resistant cells and significantly reduced cisplatin-induced early apoptosis, although it had no notable effect on cell proliferation. Moreover, the study showed that MEOX2 was not associated with immune cell infiltration in OV but was positively correlated with angiogenesis-related genes. In cisplatin-resistant cells, gene set enrichment analysis of MEOX2 co-expressed genes highlighted the activation of the E2F target and DNA repair pathway. Additionally, MEOX2 exhibited a significant negative correlation with the MCM protein family. In summary, MEOX2 is highly expressed in OV and is associated with poor patient prognosis. It may confer cisplatin resistance to OV cells by activating the E2F target and DNA repair pathway to mitigate cisplatin-induced early apoptosis. Despite certain limitations, these findings provide novel insights into the potential role of MEOX2 as a prognostic biomarker and therapeutic target in OV.

Keywords Ovarian cancer, MEOX2, Prognosis, Cisplatin resistance, Transcriptomic analysis

*Correspondence:
Hui Yang
kittyyh@nwpu.edu.cn
[1]School of Life Sciences, Northwestern Polytechnical University, Xi'an 710072, Shaanxi, China
[2]Engineering Research Center of Chinese Ministry of Education for Biological Diagnosis, Treatment and Protection Technology and Equipment, Xi'an 710072, Shaanxi, China
[3]Research Center of Special Environmental Biomechanics & Medical Engineering, Northwestern Polytechnical University, Xi'an 710072, Shaanxi, China
[4]Department of Gynecology, Shaanxi Provincial People's Hospital, Xi'an 710068, Shaanxi, China

Introduction

Ovarian cancer (OV) is the most lethal gynecological malignancy, posing a significant global threat to women's health [1]. In 2019, millions of new cases were reported worldwide, resulting in hundreds of thousands of deaths due to disease progression [2]. Clinically, most OV cases are diagnosed at an advanced stage [3], with cancer cells exhibiting a high propensity for metastasis to organs such as the fallopian tubes, uterus, and intestines, complicating prognosis and treatment outcomes [4]. Standard treatment involves cytoreductive surgery followed by a dual chemotherapy regimen comprising platinum and taxane agents, which induce remission in over 50% of advanced-stage cases [5]. However, the high recurrence rate—affecting approximately 70% of advanced-stage patients within 18 months—presents a critical challenge, with nearly 50% succumbing to the disease within five years of initial diagnosis [6]. This highlights an urgent need for innovative therapeutic approaches to prolong remission and improve survival rates.

Cisplatin, a platinum-based chemotherapeutic agent that disrupts DNA replication and transcription, remains a cornerstone in cancer treatment [7, 8]. Despite its efficacy, the emergence of cisplatin resistance represents a formidable obstacle, prompting the development of strategies such as combining cisplatin with adjunctive agents (e.g., paclitaxel, berberine, resveratrol) [9–11] and utilizing advanced drug delivery systems to enhance therapeutic efficacy and minimize toxicity [12]. Another promising strategy involves targeting resistance-related genes to combat cisplatin resistance.

Mesenchyme Homeobox 2 (MEOX2), a nuclear transcription factor initially identified for its role in inhibiting the growth of vascular smooth muscle and endothelial cells, has been implicated as a tumor-initiating factor in glioma [13]. Studies have shown that MEOX2 contributes to tumor growth, metastasis, drug resistance, and poor prognosis in various cancers, including hepatocellular carcinoma, cervical cancer, and breast cancer [14–16]. However, its role in OV remains largely unexplored. This study addresses the pressing issues of OV diagnosis and cisplatin resistance by leveraging bioinformatics analyses to identify key targets associated with OV onset, prognosis, and drug resistance. The identified targets are further investigated through mechanistic predictions and rigorous biological validation.

Results

Identification and pathway enrichment analysis of dual differentially expressed genes (DEGs) associated with tumorigenesis and cisplatin resistance

To identify key genes involved in OV prognosis and drug resistance, we integrated data from The Cancer Genome Atlas (TCGA) and Genotype-Tissue Expression (GTEx) databases to analyze transcriptomic profiles of OV tissues and corresponding normal adjacent tissues. Following data standardization and integration, principal component analysis (PCA) revealed significant spatial separation between tumor and normal tissues (Fig. 1A). Differential expression analysis identified 3,187 upregulated and 4,944 downregulated DEGs in OV tissues compared to normal tissues ($|Log_2FC| \geq 1$ & FDR < 0.05) (Fig. 1B). Previous studies have demonstrated that aberrant gene expression in cancer cells can exacerbate resistance to platinum-based chemotherapeutics, complicating treatment outcomes. To further investigate cisplatin resistance, we analyzed the GSE15372 dataset, which revealed substantial differences between cisplatin-resistant and sensitive strains. Differential expression analysis identified 945 DEGs associated with cisplatin resistance, comprising 426 upregulated and 519 downregulated genes (Fig. 1C-D). Integrating these DEGs with those identified from OV tissues resulted in 461 overlapping DEGs (Fig. 1E), suggesting a potential collaborative role in both tumorigenesis and cisplatin resistance.

The Kyoto Encyclopedia of Genes and Genomes (KEGG) pathway enrichment analysis revealed that these 461 DEGs are predominantly involved in cancer-related pathways (e.g., pathways in cancer, prostate cancer), cell proliferation (e.g., PI3K-Akt signaling pathway, MAPK signaling pathway, cell cycle), cell adhesion (e.g., cell adhesion molecules), and inflammation-related pathways (e.g., cytokine-cytokine receptor interaction, IL-17 signaling pathway) (Fig. 1F).

Screening for DEGs significantly associated with OV survival

In continuation of our efforts to identify key genes associated with prognosis and drug resistance in OV, we conducted Cox univariate analysis was conducted to identify DEGs significantly associated with OV survival. Cox univariate analysis was performed to identify DEGs significantly correlated with OV survival, identifying 30 DEGs with prognostic significance (Fig. 2A). Random forest analysis further prioritized four key genes (MEOX2, GBP1, PSMB8, and ANXA10) as potential prognostic markers (Fig. 2B-C).

MEOX2 correlation with prognosis and increased expression with disease stage

We evaluated the prognostic significance of MEOX2 using clinical data from the TCGA database. Kaplan-Meier analysis showed that MEOX2 expression was positively correlated with overall survival in OV patients (HR = 1.664; $P = 0.0004$), while GBP1 demonstrated an inverse correlation (HR = 0.6910; $P = 0.0096$) Fig. 3A). Expression analysis across OV stages revealed significantly higher MEOX2 levels in stages III and IV

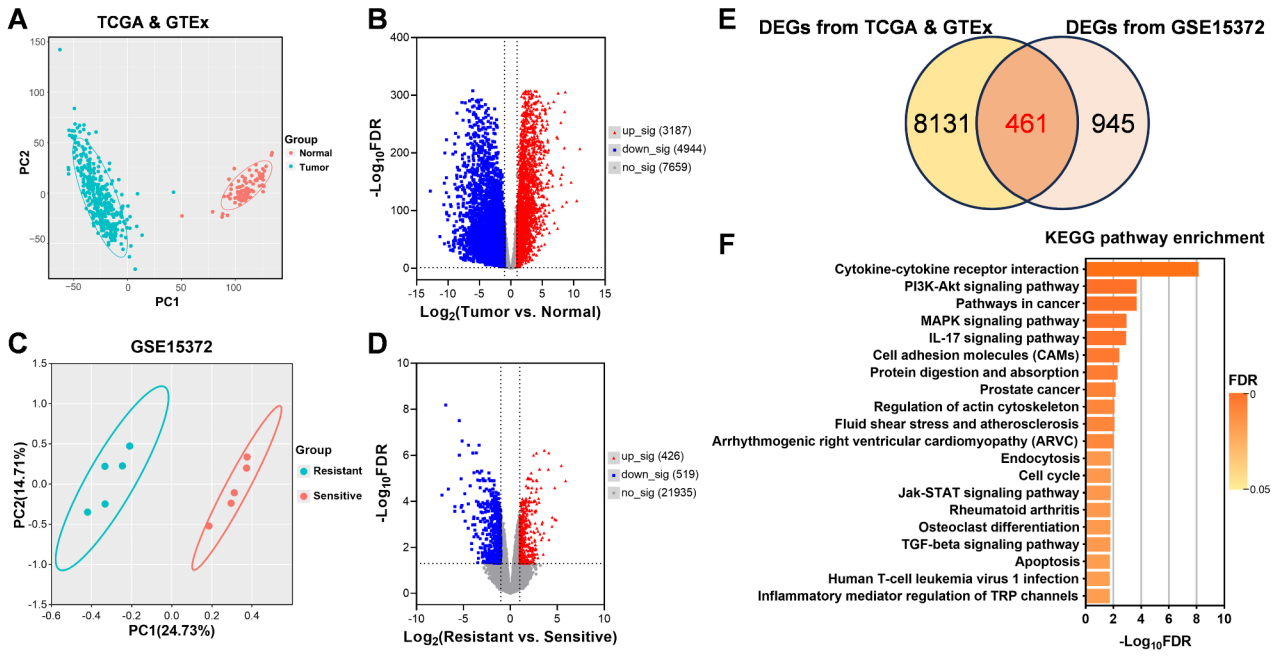

Fig. 1 Screening of dual genes for OV occurrence and drug resistance. (**A**) PCA of the expression profiles of tumor and normal tissues. (**B**) DEGs between tumor and normal tissues. (**C**) PCA of cisplatin-sensitive and cisplatin-resistant cells in GSE15372 dataset. (**D**) DEGs between cisplatin-sensitive and cisplatin-resistant cells. (**E**) The Venn diagram of DEGs. (**F**) KEGG pathway analysis of intersecting genes

compared to stage II ($P < 0.05$) (Fig. 3B). These findings suggest that MEOX2 expression is stage-dependent and prognostically relevant, prompting further validation of its role as a key survival-associated gene.

Tissue microarray analysis validates high MEOX2 expression and its clinical relevance

Immunohistochemical (IHC) analysis of OV tissue microarrays confirmed high MEOX2 expression in tumor samples (Fig. 4A-B). Survival analysis revealed that higher MEOX2 expression correlated with shorter overall and disease-free survival (Fig. 4C). Furthermore, Cox analysis demonstrated a positive correlation between MEOX2 expression and tumor size and staging (Fig. 4D, Table 1). Collectively, these results underscore the clinical relevance of MEOX2 as a key driver in OV progression.

MEOX2 expression in cisplatin-resistant cells and its functional role

To validate MEOX2 expression in cisplatin-resistant cells, we assessed its levels in various cell lines using The Human Protein Atlas (HPA; https://www.proteinatlas.org/) database. Among eight cell lines expressing MEOX2, A2780 exhibited the highest expression, prompting its selection for further experiments (Fig. 5A). Cisplatin sensitivity assays showed that A2780-DDP cells exhibited higher resistance (IC50 = 66.55 μM) compared to parental A2780 cells (Fig. 5B). qPCR and Western blot analyses revealed significantly higher MEOX2 expression in A2780 cells compared to normal ovarian epithelial cells (IOSE-80) Fig. 5C-D). However, upon acquiring cisplatin resistance, MEOX2 levels decreased in A2780-DDP cells, although they remained higher than in IOSE-80 cells (Fig. 5C-D).

To further investigate the role of MEOX2 in cisplatin resistance in OV, we silenced MEOX2 in cisplatin-resistant cells. As shown in Fig. 5E, qPCR results revealed that siRNA-1013 achieved the highest knockdown efficiency for MEOX2 and was subsequently selected for further experiments. Knockdown of MEOX2 using siRNA further enhanced cisplatin resistance in A2780-DDP cells (IC50 = 96.44 μM) (Fig. 5F-G). Additionally, cell proliferation was significantly inhibited in resistant cells, both with and without cisplatin treatment, after MEOX2 knockdown. To better assess the impact of MEOX2 knockdown on cisplatin resistance, we calculated the proliferation ratio between cisplatin-treated (DDP) and untreated (NC) groups to evaluate the relative inhibitory effect of cisplatin on cell proliferation or viability. The results showed that cisplatin treatment significantly suppressed proliferation in A2780 cells, while its inhibitory effect was markedly attenuated in A2780-DDP cells. However, no significant changes were observed upon MEOX2 knockdown in the resistant cells (Fig. 5H). Apoptosis assays revealed that, in the absence of cisplatin treatment, all groups exhibited low apoptosis rates with no significant differences. Under cisplatin treatment, the total apoptosis rate of A2780-DDP cells was significantly

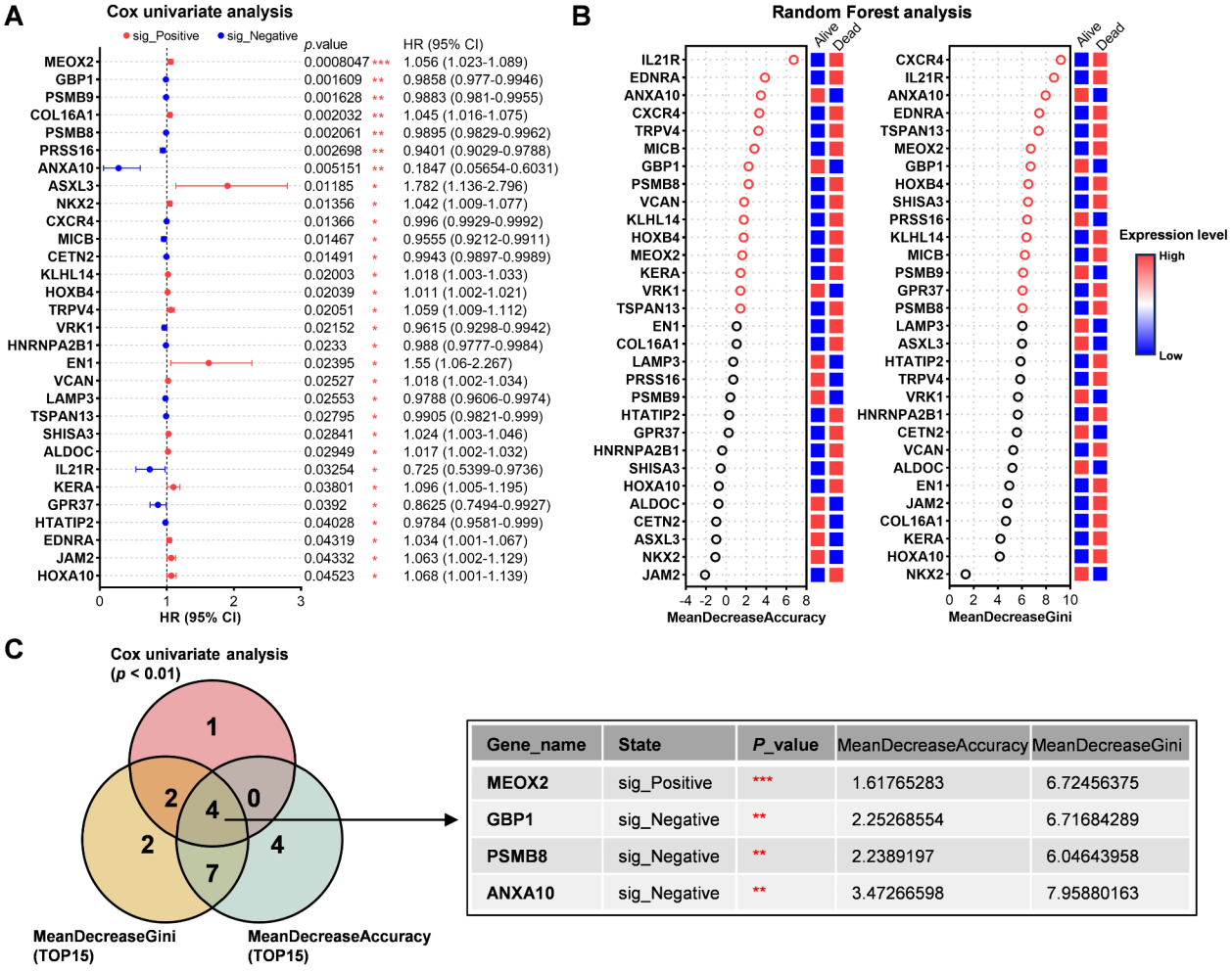

Gene_name	State	*P*_value	MeanDecreaseAccuracy	MeanDecreaseGini
MEOX2	sig_Positive	***	1.61765283	6.72456375
GBP1	sig_Negative	**	2.25268554	6.71684289
PSMB8	sig_Negative	**	2.2389197	6.04643958
ANXA10	sig_Negative	**	3.47266598	7.95880163

Fig. 2 Screening for key genes for OV survival. (**A**) Cox univariate analysis of DEGs. (**B**) Random forest model prediction of DEGs significantly associated with survival. (**C**) Venn diagram for the selection of core genes associated with survival in OV

lower than that of A2780 cells, and this reduction became even more pronounced following MEOX2 knockdown (Fig. 5I). Further analysis indicated that both early and late apoptosis ratios were significantly reduced in resistant cells after MEOX2 silencing. However, only the reduction in early apoptosis showed statistical significance when relative apoptosis rates (DDP/NC) were calculated. Finally, wound healing assays demonstrated that the migratory ability of resistant cells was significantly impaired following MEOX2 knockdown (Fig. 5J). These findings collectively highlight the critical role of MEOX2 in cisplatin-resistant cells. Its silencing further enhances the resistance of these cells to cisplatin, primarily by increasing their ability to evade cisplatin-induced early apoptosis.

MEOX2 is associated with angiogenesis-related genes but not immune cell infiltration

The tumor microenvironment, particularly the degree of immune cell infiltration, has been shown to influence tumor growth and response to treatment by modulating immune responses. Analysis of the OV tumor microenvironment revealed no significant correlation between MEOX2 expression and immune cell infiltration (Fig. 6A). In addition to immune cell infiltration, angiogenesis is another crucial factor in the microenvironment. However, MEOX2 showed a significant positive correlation with angiogenesis-related genes, including POSTN, LUM, COL3A1, COL5A2, and VCAN ($P < 0.05$ &$|R| > 0.5$) (Fig. 6B-C). These findings suggest that MEOX2 may influence OV progression through angiogenic mechanisms.

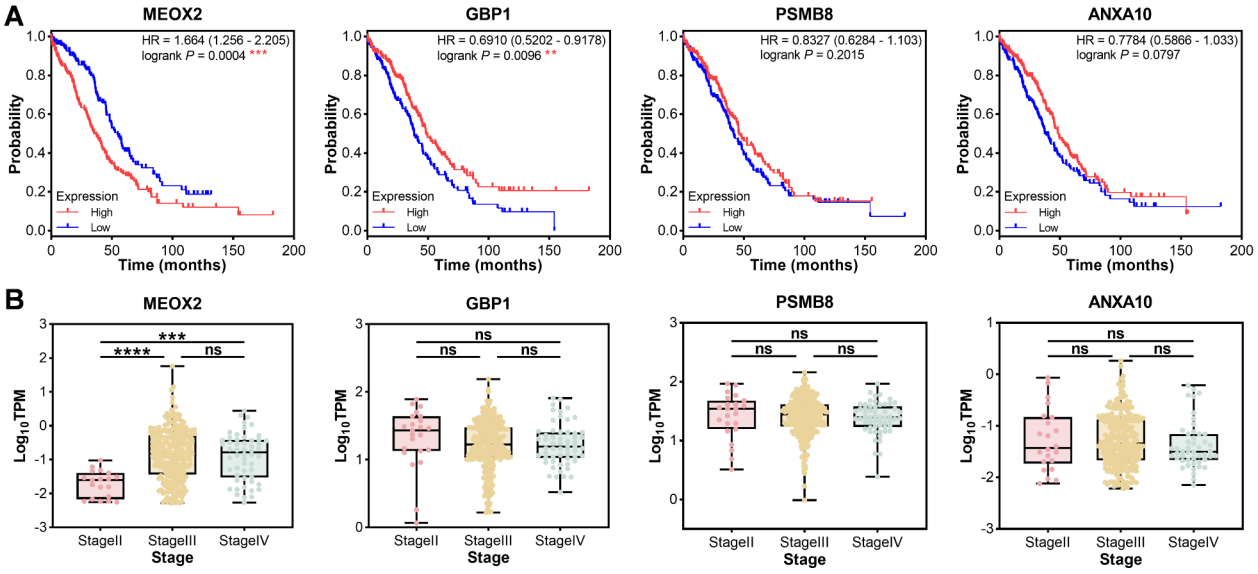

Fig. 3 The expression of key genes is associated with both the survival and staging of OV. (**A**) Survival prognosis analysis. (**B**) Gene expression levels across different stages of OV

Gene set enrichment analysis (GSEA) analysis of MEOX2 co-expressed genes in drug-resistant OV cells

To explore potential pathways regulated by MEOX2, GSEA was performed on its co-expressed genes in drug-resistant cells. Using the GSE15372 dataset, we calculated Spearman correlation coefficients between MEOX2 and other genes, obtaining a total of 2909 co-expressed genes (1777 positively correlated and 1132 negatively correlated; $P < 0.05$ &$|R| \geq 0.75$). Analysis identified significant enrichment of 22 pathways, primarily involving energy metabolism (e.g., oxidative phosphorylation, glycolysis), DNA replication (e.g., G2M checkpoint, DNA repair), and signaling pathways (e.g., E2F targets) (Fig. 7A-B). Within the E2F pathway (ES = 0.615, FDR < 0.0001; Fig. 7B), the majority of enriched genes were upregulated, including highly interactive nodes such as MCM4, MCM6, MCM7, MCM5, RRM2, MCM2, and SMC4 (Fig. 7C-D). These pathways may underpin MEOX2's role in drug resistance.

Discussion

remains one of the most significant threats to women's health, ranking as one of the leading causes of malignancy-related mortality worldwide. While platinum-based chemotherapy has achieved notable success in treating OV, the emergence of cisplatin resistance has severely compromised its therapeutic efficacy [17]. Therefore, elucidating the molecular mechanisms underlying cisplatin resistance is critical for improving patient outcomes. Advances in bioinformatics analysis have provided powerful tools for identifying novel biomarkers and therapeutic targets, offering fresh perspectives on OV pathogenesis and therapeutic resistance [18, 19]. However, due to the complexity and heterogeneity of OV, there remains an urgent need to identify more effective therapeutic targets to enhance survival rates and improve treatment outcomes. In this study, we utilized bioinformatics tools, tissue microarrays, and cellular experiments to identify and validate MEOX2 as a gene associated with both prognosis and cisplatin resistance in OV. Our findings revealed that MEOX2 plays a pivotal role in OV progression and drug resistance. High expression of MEOX2 was strongly correlated with poor survival outcomes in OV patients, underscoring its potential as a prognostic biomarker. Intriguingly, although MEOX2 expression was significantly reduced in cisplatin-resistant cells, its functional silencing further enhanced cisplatin resistance. This paradoxical result suggests that MEOX2 may have distinct roles in regulating cisplatin sensitivity depending on its expression context.

We found that silencing MEOX2 in resistant cells significantly increased the IC50 value of cisplatin, indicating heightened resistance to the drug. However, contrary to expectations, MEOX2 knockdown did not enhance cell proliferation in resistant cells, regardless of cisplatin treatment. Instead, cisplatin-induced early apoptosis was significantly reduced following MEOX2 silencing, suggesting that MEOX2 contributes to cisplatin sensitivity primarily by modulating apoptosis pathways. Collectively, these findings indicate that MEOX2 enhances cisplatin sensitivity in resistant cells by promoting early apoptosis rather than by directly affecting cell proliferation. In addition, wound-healing assays revealed that the migratory ability of resistant cells was significantly

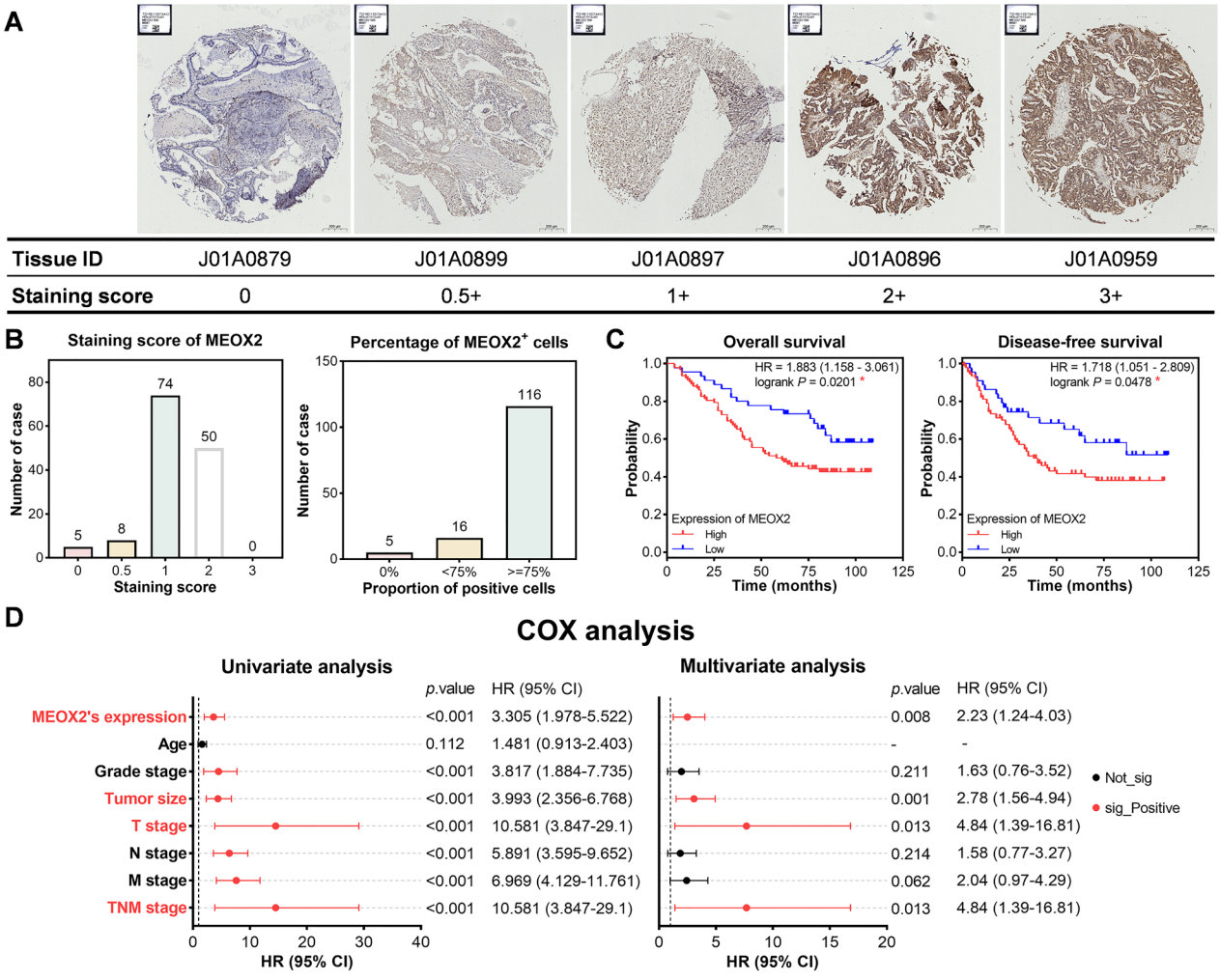

Fig. 4 The expression of MEOX2 in OV tissue microarrays and its correlation with clinical data. (**A**) Representative images of positive staining and corresponding scoring (scale bar = 200 μm). (**B**) Positive staining score and cell proportion. (**C**) Survival curves of overall survival and disease-free survival for patients with MEOX2. (**D**) Cox analysis of MEOX2 with clinical data

Table 1 Correlation analysis between MEOX2 expression and clinical data in tissue chips

	variable	MEOX2 expression		total	*P-value*	*r-value*
		low	high			
Age (year)	≤ 51	36	32	68	0.863	0.029
	> 51	33	33	66		
Grade	I/II	22	12	34	0.014	0.242
	III	29	46	75		
Tumor size	≤ 12.2 cm	42	27	69	0.025	0.2
	> 12.2 cm	27	39	66		
T stage	T1/T2	25	16	41	0.138	0.132
	T3	43	49	92		
N stage	N0	56	43	99	0.046	0.186
	N1	12	22	34		
M stage	M0	60	45	105	0.01	0.233
	M1	8	20	28		
TNM stage	I/II	25	16	41	0.138	0.132
	III/IV	43	49	92		

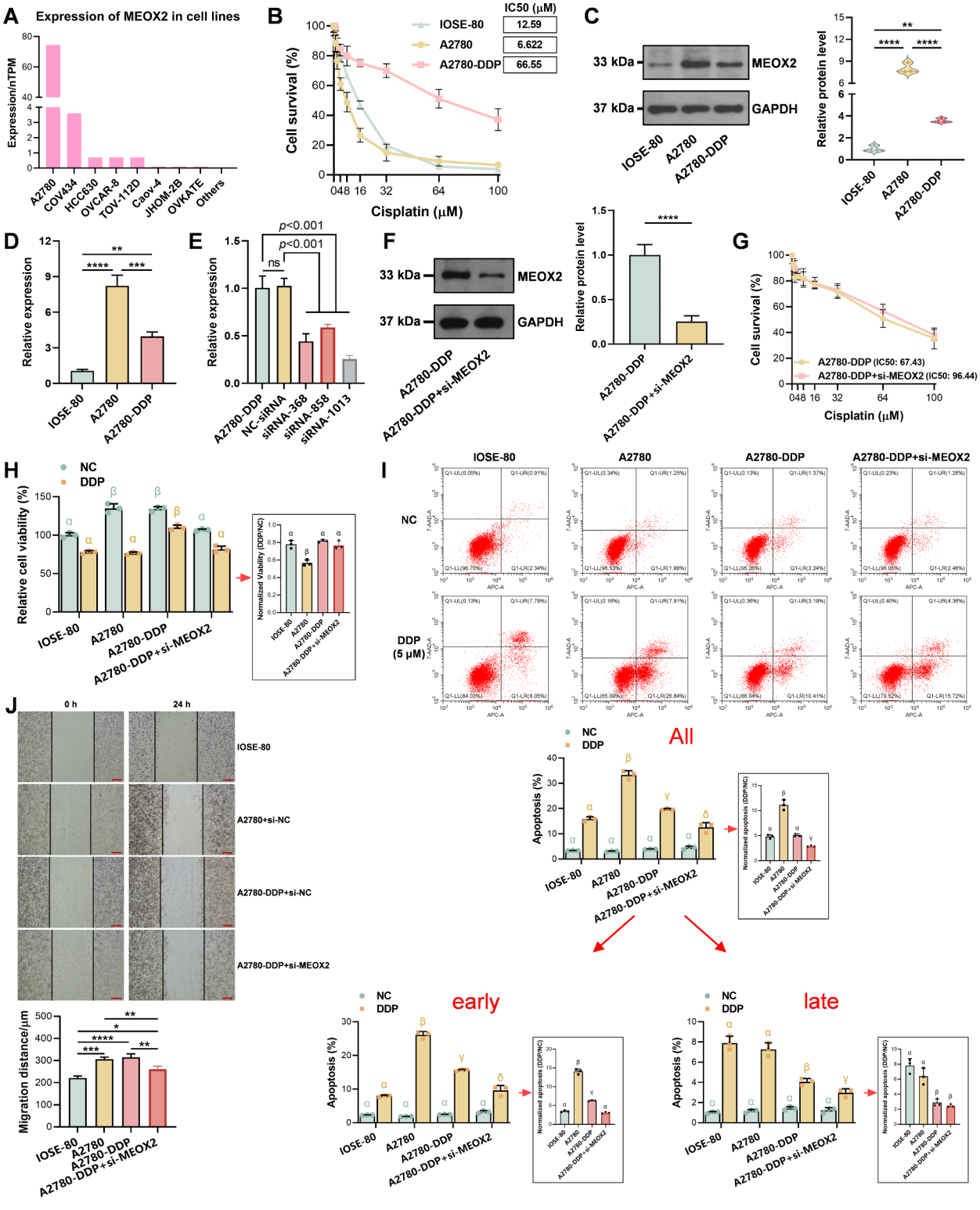

Fig. 5 (See legend on next page.)

(See figure on previous page.)

Fig. 5 In vitro validation of MEOX2 expression levels and function. (**A**) MEOX2 expression levels in different cell lines based on the HPA database. (**B**) The sensitivity of IOSE-80, A2780, and A2780-DDP cells to cisplatin was evaluated using the CCK-8 assay, and IC50 values were calculated for comparison. (**C**) MEOX2 protein expression in IOSE-80, A2780, and A2780-DDP cells was evaluated by Western blot analysis. (**D**) The relative mRNA expression levels of MEOX2 in A2780 and A2780-DDP cells were determined by qPCR, normalized to the expression levels in IOSE-80 cells. (**E**-**F**) The knockdown efficiency of MEOX2 in A2780-DDP cells was validated by qPCR (**E**) and Western blot (**F**), showing changes in mRNA and protein expression. (**G**) The impact of MEOX2 knockdown on cisplatin sensitivity in A2780-DDP cells was evaluated, as reflected by changes in IC50 values. (**H**) Cell viability was measured in different groups treated with 5 μM cisplatin (DDP) or untreated (NC), normalized to the viability of IOSE-80 cells. The inset graph illustrates the effects of cisplatin treatment on cell viability, excluding interference from initial viability differences among groups. (**I**) Apoptosis rates in different cell groups were analyzed using flow cytometry after cisplatin treatment, including total apoptosis (All apoptosis), early apoptosis (Early apoptosis), and late apoptosis (Late apoptosis). (**J**) The effect of MEOX2 knockdown on the migratory ability of A2780-DDP cells was assessed using a wound healing assay, comparing migration distances at 0 h and 24 h (scale bar = 100 μm; labelled as a red line). All experiments were performed in triplicate, and data are presented as mean ± standard deviation (Mean ± SD). For statistical annotations in Figures H and I, Greek letters (α, β, γ, δ) of the same color represent the groups being compared, with different letters indicating statistically significant differences between groups

impaired after MEOX2 silencing. This result highlights the complex and multifaceted role of MEOX2 in OV progression and drug resistance.

Using public datasets, we initially identified 461 DEGs potentially associated with OV prognosis and cisplatin resistance. Pathway enrichment analysis revealed that these DEGs were involved in inflammatory signaling pathways, such as the IL-17 signaling pathway. IL-17 is an inflammatory cytokine involved in OV pathogenesis by regulating inflammatory responses, enhancing the inflammatory state of the tumor microenvironment, and promoting tumor cell proliferation and metastasis [20–23]. Recent studies have shown that IL-17 accelerates OV cell growth and infiltration by promoting the polarization and activation of tumor-associated macrophages [24]. Additionally, IL-17 induces the expression of matrix metalloproteinases in tumor cells, facilitating tumor cell invasion and metastasis [25]. We also investigated the correlation between MEOX2 and immune cell infiltration in OV, finding a low correlation, suggesting that inflammatory infiltration in OV might be regulated by other DEGs, warranting further study.

Some studies suggest that MEOX2 can inhibit endothelial cell proliferation and angiogenesis in vitro and in vivo models [26–28]. It is widely accepted that hypoxia within tumors can activate hypoxia-inducible factor-mediated angiogenesis [29]. Increased neovascularization within tumors facilitates tumor proliferation, invasion, and migration, making the condition difficult to control [30]. We analyzed the correlation between MEOX2 and angiogenesis-related gene sets in OV, identifying a significant positive correlation between MEOX2 expression and five angiogenesis-related genes: POSTN, LUM, COL3A1, COL5A2, and VCAN. POSTN (Periostin) is a component of the extracellular matrix, shown to promote new blood vessel formation via the Erk/VEGF pathway, and is involved in tumor cell proliferation, progression, migration, and epithelial-mesenchymal transition [31]. Feng et al. indicated that LUM serves as a marker for cancer-associated fibroblast infiltration and is linked to poor prognosis in high-risk OV patients [32]. COL5A2, part of the collagen family, is overexpressed in various epithelial cancers, and its inhibition reduces cell proliferation and invasion [33]. VCAN (Versican) overexpression correlates with increased vascular density and invasive potential in OV tumors [34]. We hypothesize that MEOX2 may promote OV progression by influencing angiogenesis.

Further, we used GSEA to explore the potential mechanisms by which MEOX2 mediates cisplatin resistance in OV. Our analysis revealed activation of pathways related to energy metabolism and DNA replication in resistant cells. Additionally, the E2F targets was significantly enriched in MEOX2-expressing cells. Cisplatin exerts its effects by binding to DNA and forming DNA adducts, leading to DNA damage, including interstrand cross-links, which obstruct DNA replication and transcription, thereby inducing apoptosis [35]. Enhanced DNA repair capacity can increase genomic stability, enabling cells to better cope with cisplatin-induced DNA damage [36]. Consistently, we found that genes co-expressed with MEOX2 in cisplatin-resistant cells activated DNA repair pathways. The E2F targets pathway involves E2F family members and a series of genes regulated by them, playing crucial roles in DNA replication, cell cycle progression, DNA repair, apoptosis, and cell metabolism [37, 38]. Moreover, seven genes, including MCM4, MCM6, MCM7, MCM5, RRM2, MCM2, and SMC4, were identified as hub genes, significantly negatively correlated with MEOX2 and upregulated in cisplatin-resistant cells. The Minichromosome Maintenance (MCM) family proteins are crucial for the initiation of DNA replication and maintaining genomic stability. Studies have shown that abnormal expression of MCM proteins in OV is closely related to chemotherapy resistance. The MCM2-7 protein complex plays a key role in initiating DNA replication. Overexpression of MCM proteins can protect cancer cells from chemotherapy-induced replication stress, leading to drug resistance [39]. Altered phosphorylation states of MCM2 and MCM4 can affect their functions during replication initiation and elongation, potentially enabling OV cells to escape chemotherapy-induced cell cycle arrest, leading to resistance [40]. Thus, while MEOX2 expression is downregulated in resistant cells, it may facilitate cisplatin resistance by activating

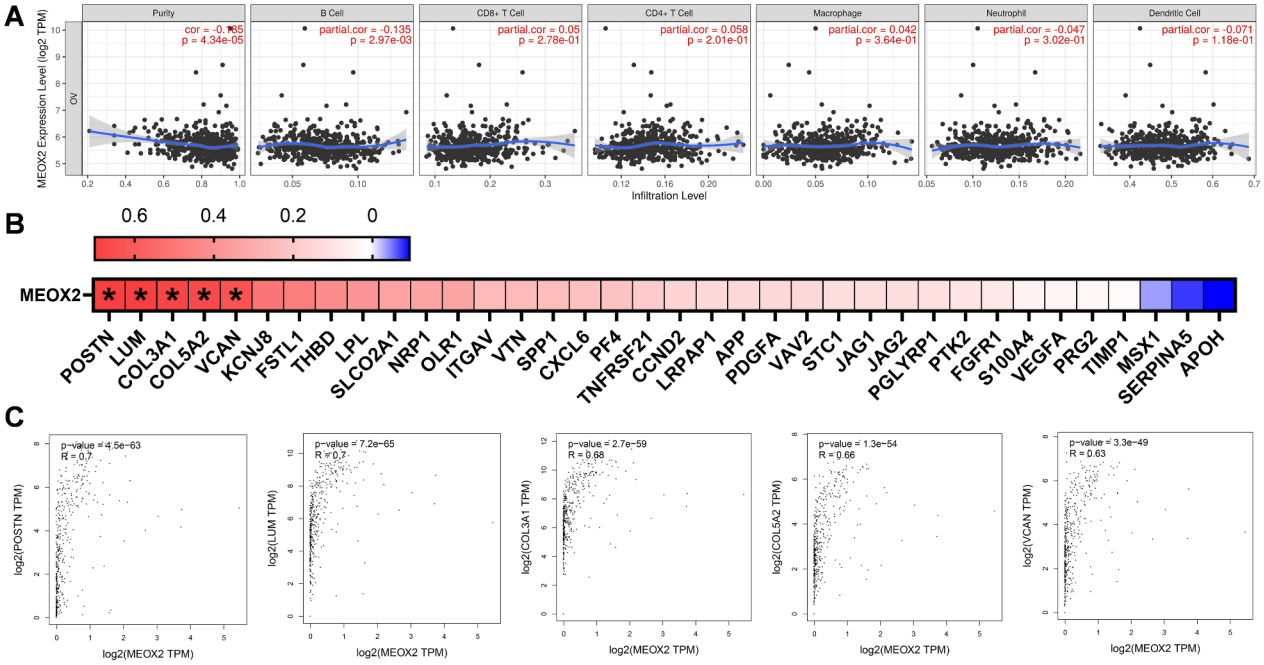

Fig. 6 MEOX2 and its relationship with the tumor microenvironment. (**A**) Correlation analysis between MEOX2 and immune cell infiltration in OV. (**B**) Correlation analysis between MEOX2 and angiogenesis-related genes. (**C**) Correlation analysis plot of genes significantly correlated with MEOX2

DNA repair and E2F target pathways, enabling cells to evade cisplatin-induced DNA damage and apoptosis.

While our study provides valuable insights into the role of MEOX2 in OV progression and cisplatin resistance, several limitations must be acknowledged. (1) While we demonstrated the role of MEOX2 using siRNA-mediated knockdown experiments, complementary overexpression studies would further validate its functional mechanisms. (2) Although in vitro experiments provided strong evidence, in vivo studies using animal models would be beneficial to better capture the tumor microenvironment and systemic interactions. (3) The study cohorts used in our analysis may not fully represent the global OV patient population. Validation in larger and more diverse cohorts would enhance the generalizability of our findings. Despite these considerations, the findings of this study establish MEOX2 as a promising prognostic biomarker and therapeutic target in OV. Future research will aim to build on these results and further explore the therapeutic potential of targeting MEOX2 to overcome cisplatin resistance and improve patient outcomes.

In summary, our study highlights MEOX2 as a critical regulator of cisplatin resistance and progression in OV. High MEOX2 expression is associated with poor patient prognosis, while its silencing enhances cisplatin resistance by reducing cisplatin-induced early apoptosis. Mechanically, MEOX2 contributes to resistance through activation of the E2F target and DNA repair pathways and may also promote OV progression by influencing angiogenesis-related pathways. These findings underscore the potential of MEOX2 as both a prognostic biomarker and a therapeutic target in OV, providing a foundation for future studies aimed at improving outcomes for OV patients.

Materials and methods

Data collection and standardization

To identify potential pathogenic genes in OV, mRNA expression profile data for TCGA-OV (379 OV samples) and GTEx (88 control samples) were downloaded from the UCSC XENA (https://xena.ucsc.edu/) database. The two datasets were merged, and data preprocessing was performed using the R packages "DESeq2" and "sva", which included log transformation to counts and removal of batch effects. The standardized dataset was utilized for subsequent analyses.

Analysis of potential pathogenic genes in OV

Differential analysis between OV samples and control samples was performed using the R package 'edgeR' with a threshold for selecting DEGs set at $|\mathrm{Log_2FC}| \geq 1$ & FDR < 0.05. Additionally, PCA was conducted on the merged data using the 'prcomp' function, and visualization was carried out using the R package 'ggplot2' to distinguish between cancer and normal samples.

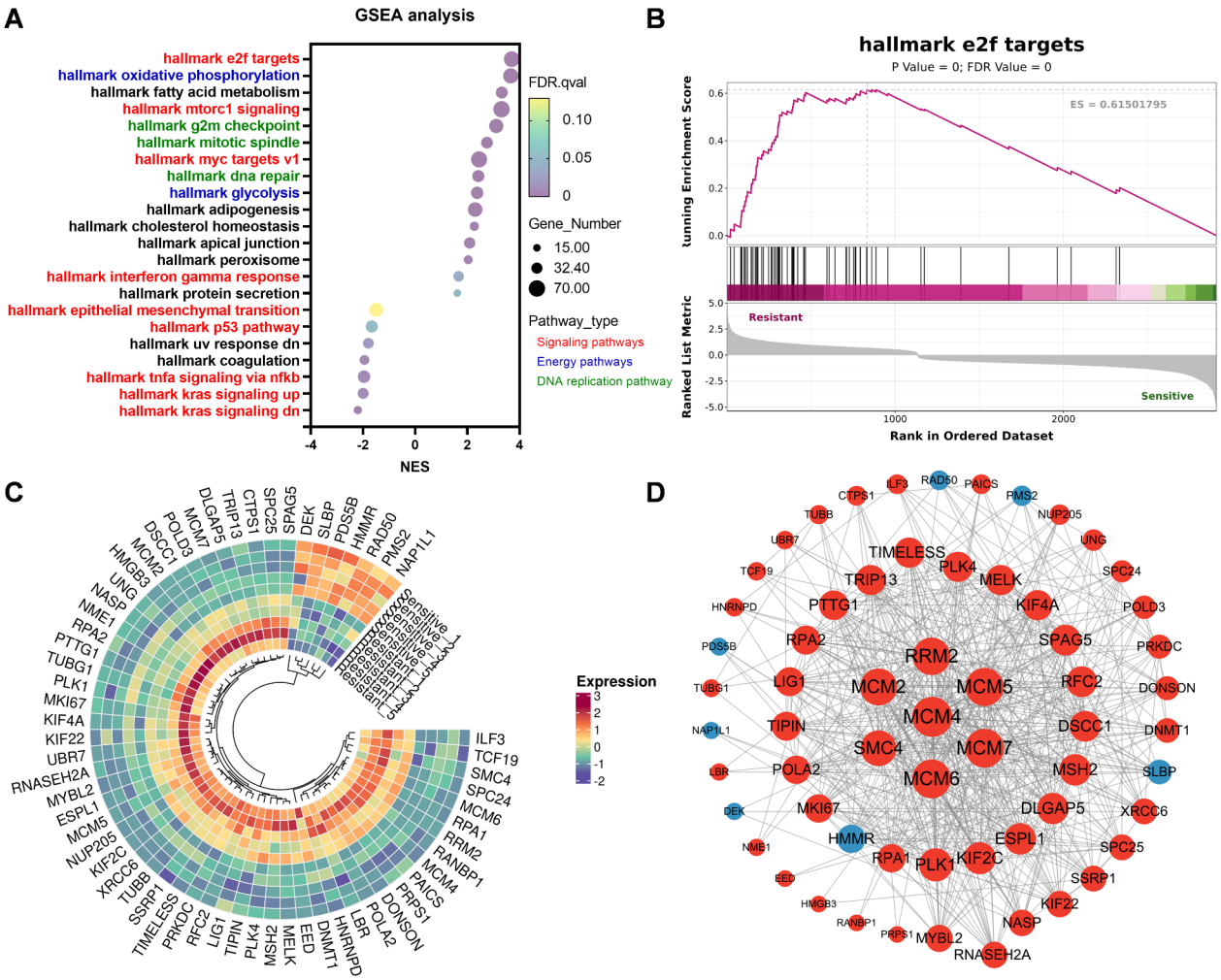

Fig. 7 GSEA analysis involved in co-expressed genes with MEOX2 in cisplatin-resistant cells. (**A**) GSEA enrichment analysis of MEOX2 co-expressed genes. (**B**) GSEA analysis showing activation of the E2F targets pathway in resistant cells. (**C**-**D**) Differential distribution of enriched genes in the E2F targets pathway between resistant and sensitive OV cells (**C**) and their PPI network analysis (**D**). Targets up-regulated in resistant cells are indicated as red nodes and down-regulated targets are indicated as blue nodes

Screening of genes associated with OV cisplatin resistance

The Gene Expression Omnibus (GEO; https://www.ncbi.nlm.nih.gov/geo/), an open database, was utilized to acquire cisplatin resistance datasets for OV. We selected the GSE15372 dataset for screening genes associated with cisplatin resistance in OV. PCA was employed to distinguish between groups of samples, and potential genes for cisplatin resistance (adjusted $P\text{-}value < 0.05, |\mathrm{Log_2FC}| \geq 1$) were identified using the R package "limma". The obtained results were visualized using the R package "ggplot2".

Selection of dual genes associated with prognosis and cisplatin resistance

We selected the intersection of the identified potential pathogenic genes in OV and the genes associated with cisplatin resistance for further analysis. Using cancer sample data, along with survival status (OS.status) and survival time (OS.time) data, we conducted batch Cox univariate survival analysis on the common DEGs using the R packages 'survival' and 'survminer'. Subsequently, GAPtools (https://www.gaptools.cn/#/tool) were employed for random forest screening of genes that significantly influenced survival analysis. The parameters used were mtry = 2 and ntree = 1000. Genes were then selected based on a threshold of MeanDecreaseGini > 25, resulting in key genes. Expression difference heatmaps and corresponding survival curves for these key genes were separately generated for groups with long and short survival times.

Tissue microarray detection

In this study, we utilized an OV tissue microarray (HOvaC151Su01) obtained from Shanghai Outdo Biotech Co.,

Ltd., which contains 150 well-characterized OV samples, each accompanied by detailed clinical information, including patient age, gender, cancer staging, and prognosis. The primary aim of this study is to investigate the expression of MEOX2 in OV and its clinical significance. To achieve this, IHC staining was performed on the tissue samples. The selected tissue sections containing OV were first subjected to standard fixation and embedding procedures. Subsequently, a standard IHC protocol was applied to assess the expression of MEOX2 in the tissue samples. The interpretation of staining results followed this procedure: at low magnification, the overall staining intensity of each tissue point was evaluated and categorized as weakly positive (1), moderately positive (2), or strongly positive (3). In cases where different staining intensities were observed within the same tissue point, a mixed score (e.g., 2–3) was used. High magnification was then applied to select three areas with varying staining intensities. In each of these areas, 100 cells were randomly selected, and the percentage of positive cells was calculated to determine the positivity rate for each field. Finally, the staining intensity score was multiplied by the positivity rate score to obtain a total score (0-300%) for each tissue point. Based on the total MEOX2 expression score, samples were classified into low-expression group (total score ≤ 142.5%) and high-expression group (total score > 142.5%), with 142.5% representing the median total score of all samples. Using this analytical approach, we further investigated the relationship between MEOX2 expression and clinical parameters (such as cancer staging and prognosis), including survival analysis, univariate and multivariate Cox regression analyses, and correlation analysis based on Fisher's test.

Cell culture and treatment

The ovarian epithelial control cell lines (IOS-80), OV cell line A2780 and its cisplatin-resistant counterpart A2780-DDP were provided by the Department of Gynecology, Shaanxi Provincial People's Hospital. A2780 cells were cultured in DMEM/F-12 medium (Procell, Wuhan, China) supplemented with 10% fetal bovine serum (FBS), while other cells were cultured in RPMI 1640 medium (Procell, Wuhan, China) supplemented with 10% FBS. All media were supplemented with 1% penicillin-streptomycin solution (Procell, Wuhan, China). Cells were maintained at 37 °C in a humidified atmosphere containing 5% CO_2 and subcultured when reaching 80% confluence.

Cells in logarithmic growth phase and good condition were seeded at a density of 5×10^5 cells per well in 6-well culture plates and incubated overnight at 37 °C with 5% CO_2. Subsequently, siRNA was diluted in serum-free OPTI-MEM (GIBCO, Thermo Fisher Scientific, Waltham, MA, USA) and incubated, followed by dilution of LipofectamineTM 2000 (Invitrogen, Carlsbad, CA, USA) and incubation. After mixing the two solutions, they were added to the culture plates. After 6 h of transfection, the medium was replaced with fresh complete medium, and cells were continued to be cultured at 37 °C with 5% CO_2. After transfection, the silencing efficiency of siRNA targeting MEOX2 was evaluated using qPCR and Western blot.

Cell proliferation rate detection

The IC50 of cisplatin for all cells was determined as follows: Cells in logarithmic growth phase were seeded at a density of 3×10^3 cells per well in a 96-well cell culture plate and incubated overnight at 37 °C with 5% CO_2. Subsequently, cisplatin at concentrations of 1, 2, 4, 8, 16, 32, 64, and 100 μM was added to the wells. After further incubation, cell proliferation was assessed using the CCK8 assay kit (APExBIO, Houston, TX, USA). IC50 values were calculated based on the concentration-response curves generated from the assay data, representing the cisplatin concentration required for 50% inhibition of cell viability. We also assessed cell proliferation. The cell proliferation rate was measured 24 h post-transfection to evaluate the impact of siRNA on cell growth.

Cell apoptosis detection

Cell apoptosis was analyzed using an Annexin V-FITC/PI apoptosis detection kit (Qisai Biotechnology Co., Ltd., Wuhan, China) according to the manufacturer's protocol. Cells in the logarithmic growth phase were seeded in 6-well plates at a density of 3×10^5 cells per well. After treatment with 5 μM cisplatin after 24 h, cells were collected, washed with cold PBS, and resuspended in 1× binding buffer. Annexin V-FITC and PI were added to the suspension, and samples were incubated in the dark at room temperature for 15 min. Apoptotic cells were quantified using a flow cytometer (FACSCalibur, BD Biosciences), and data were analyzed using FlowJo software (TreeStar Inc., Ashland, OR, USA). Early apoptosis (Annexin V^+/PI^-) and late apoptosis (Annexin V^+/PI^+) populations were recorded and compared across groups.

Cell migration detection

Cell migration ability of IOS-80, A2780, A2780-DDP, as well as MEOX2-silenced A2780-DDP cells, was assessed using the scratch assay. Cells in logarithmic growth phase and good condition were seeded at a density of 5×10^5 cells per well in 6-well cell culture plates. After reaching confluence, scratches were made using a sterile pipette tip. The plates were then incubated for 24 h. Cell migration into the scratch area was recorded using microscopy.

Quantitative real-time PCR

Total RNA was extracted using TRIzol reagent (Invitrogen, Carlsbad, CA, USA) and was retro-transcribed

Table 2 Correlation analysis between MEOX2 expression and clinical data in tissue chips

Gene	Primer	Sequence (5′-3′)	PCR Products
Homo GAPDH	Forward	TCAAGAAGGTGGTGAAGCAGG	115 bp
	Reverse	TCAAAGGTGGAGGAGTGGGT	
Homo MEOX2	Forward	TCCTGTGCTCCAACTCTTCC	152 bp
	Reverse	TTCCTGGGAGTCTGAGCTGT	

to complementary DNA using Superscript IV reverse transcriptase (Takara Bio Inc., Shiga, Japan), followed by Real-time PCR analysis using the GoTaq qPCR Master Mix (Promega, Madison, WI, USA) on an ABI 7500 sequence detection system (Applied Biosystems, CA, USA). The procedures were set at 95 °C and denaturation for 5 min, then followed by 40 cycles of 95 °C for 15 s (denaturation) and 60 °C for 1 min (annealing). The mRNA expression level of target genes was determined using the $2^{-\Delta\Delta Ct}$ method and normalized by GAPDH (an internal control). Primer sequences are listed in Table 2.

Immunoblotting assays

After being lysed by RIPA lysate (Beyotime, Shanghai, China), the total cell proteins were obtained and quantified by BCA assay (Thermo Scientific, Waltham, MA, USA). Then, protein samples were separated by sodium dodecyl sulfate-polyacrylamide gel electrophoresis (SDS-PAGE, 10% acrylamide gels) and transferred to polyvinylidene difluoride membrane (0.22 μM, Millipore, Bedford, MA, USA), followed by blocking in 5% skimmed milk (1 h, room temperature). The membrane was then incubated with the primary antibodies: rabbit polyclonal anti-GAPDH (37 kDa, Hangzhou Xianzhi Biological Technology Co., Ltd., Hangzhou, China, AB-P-R 001) at a dilution of 1:1000 and rabbit polyclonal anti-MEOX2 (33 kDa, Proteintech Group, Inc, Wuhan, China, 12449-1-AP) at a dilution of 1:500. Subsequently, the membrane was incubated with HRP-conjugated secondary antibody (sheep anti-rabbit, BlotCycler™ HRP-conjugated Goat anti-Rabbit IgG, Beyotime, Shanghai, China, A0208) at a dilution of 1:10000. The targeted blottings were detected under the effect of enhanced chemiluminescence plus reagents and imaged using the FluorChem E imager (Protein Simple, San Jose, CA, USA). Protein bands were semi-quantified based on grayscale values scanned by Quantity One software.

Analysis of the tumour immune microenvironment

This study focused on immune cell infiltration and angiogenesis in the tumor immune microenvironment. The correlation between MEOX2 and multiple immune cell infiltration was analyzed online using Tumor Immune Estimation Resource (TIMER; https://cistrome.shinyapps.io/timer/). Angiogenesis-related gene sets were obtained in the MsigDB database and correlation analyses were performed based on the GEPIA 2 (http://gepia2.cancer-pku.cn/) database.$|R| \geq 0.5$ & $P < 0.05$ were considered significantly correlated.

MEOX2 co-expression gene screening and GSEA enrichment analysis

To explore the potential mechanism by which MEOX2 affects cisplatin resistance, screening of MEOX2 co-expressed genes was executed using the GSE15372 dataset. We counted the Spearman correlation coefficients between MEOX2 and the rest of the genes,$|R| \geq 0.75$ & $P < 0.05$ were included as co-expressed genes. GSEA annotation was performed using software downloaded from the website http://software.broadinstitute.org/gsea/index.jsp. The annotated gene setlist was selected at $P < 0.05$ & FDR < 0.25.

Statistical analysis

Statistical analyses were performed using GraphPad Prism 8.0 software. Data were presented as mean ± standard deviation (SD). Two-tailed Student's t test was performed to indicate the statistical difference between two groups and one-way analysis of variance (ANOVA) or Two-way ANOVA were used to compare the significant difference of multiple experimental groups. $P < 0.05$ was classified as statistically significant.

Supplementary Information

The online version contains supplementary material available at https://doi.org/10.1186/s13048-025-01641-2.

Supplementary Material 1

Acknowledgements

Special thanks to the Department of Gynecology, Shaanxi Provincial People's Hospital, for providing the cells. Gratitude also extends to the members of our research team for their assistance.

Author contributions

Conceptualization, F.W. and H.Y.; Methodology, F.W.; Visualization, H.Z. and X.L.; Investigation; F.W., H.Z., X.L. and Y.D.; Validation, F.W. and Y.D.; Writing—original draft, F.W.; Writing—review and editing, F.W. H.Z., X.L., Y.D. and H.Y.; Supervision, H.Y.; Funding acquisition, H.Y. All authors have read and agreed to the published version of the manuscript.

Funding

This research was funded by National Natural Science Foundation of China, grant number 12002285, and Natural Science Foundation of Shaanxi, grant number 2020JZ-11, 2022JQ-059.

Data availability

No datasets were generated or analysed during the current study.

Declarations

Institutional review board statement

Not applicable.

Informed consent

Not applicable.

Competing interests
The authors declare no competing interests.

Received: 11 September 2024 / Accepted: 1 March 2025
Published online: 21 March 2025

References

1. Kalamegam G, Sait KHW, Ahmed F, Kadam R, Pushparaj PN, Anfinan N, Rasool M, Jamal MS, Abu-Elmagd M, Al-Qahtani M. Human Wharton's Jelly Stem Cell (hWJSC) extracts inhibit ovarian cancer cell lines OVCAR3 and SKOV3 in vitro by inducing cell cycle arrest and apoptosis [J]. Front Oncol. 2018;8:592.
2. Mazidimoradi A, Momenimovahed Z, Allahqoli L, Tiznobaik A, Hajinasab N, Salehiniya H, Alkatout I. The global, regional and national epidemiology, incidence, mortality, and burden of ovarian cancer [J]. Health Sci Rep. 2022;5(6):e936.
3. Natoli M, Bonito N, Robinson JD, Ghaem-Maghami S, Mao Y. Human ovarian cancer intrinsic mechanisms regulate lymphocyte activation in response to immune checkpoint blockade [J]. Cancer Immunol Immunother. 2020;69(8):1391–401.
4. Zhang Q, Yan G, Lei J, Chen Y, Wang T, Gong J, Zhou Y, Zhao H, Chen H, Zhou Y, Wu L, Zhang J, Zhang X, Wang J, Li Y. The SP1-12LOX axis promotes chemoresistance and metastasis of ovarian cancer [J]. Mol Med. 2020;26(1):39.
5. Kim A, Ueda Y, Naka T, Enomoto T. Therapeutic strategies in epithelial ovarian cancer [J]. J Exp Clin Cancer Res. 2012;31(1):14.
6. Wang P, Hu Y, Qu P, Zhao Y, Liu J, Zhao J, Kong B. Protein tyrosine phosphatase receptor type Z1 inhibits the cisplatin resistance of ovarian cancer by regulating PI3K/AKT/mTOR signal pathway [J]. Bioengineered. 2022;13(1):1931–41.
7. Zielonka J, Joseph J, Sikora A, Hardy M, Ouari O, Vasquez-Vivar J, Cheng G, Lopez M, Kalyanaraman B. Mitochondria-targeted triphenylphosphonium-based compounds: syntheses, mechanisms of action, and therapeutic and diagnostic applications [J]. Chem Rev. 2017;117(15):10043–120.
8. Wang Q, Wu C, Li X, Yang D, Shi L. Cisplatin and paclitaxel co-delivery nanosystem for ovarian cancer chemotherapy [J]. Regen Biomater. 2021;8(3):rbab015.
9. Falchook G, Coleman RL, Roszak A, Behbakht K, Matulonis U, Ray-Coquard I, Sawrycki P, Duska LR, Tew W, Ghamande S, Lesoin A, Schwartz PE, Buscema J, Fabbro M, Lortholary A, Goff B, Kurzrock R, Martin LP, Gray HJ, Fu S, Sheldon-Waniga E, Lin HM, Venkatakrishnan K, Zhou X, Leonard EJ, Schilder RJ. Alisertib in combination with weekly paclitaxel in patients with advanced breast cancer or recurrent ovarian cancer: a randomized clinical trial [J]. JAMA Oncol. 2019;5(1):e183773.
10. Liu L, Fan J, Ai G, Liu J, Luo N, Li C, Cheng Z. Berberine in combination with cisplatin induces necroptosis and apoptosis in ovarian cancer cells [J]. Biol Res. 2019;52(1):37.
11. Islam SS, Aboussekhra A. Sequential combination of cisplatin with eugenol targets ovarian cancer stem cells through the Notch-Hes1 signalling pathway [J]. J Exp Clin Cancer Res. 2019;38(1):382.
12. Zhou X, Ling K, Liu M, Zhang X, Ding J, Dong Y, Liang Z, Li J, Zhang J. Targeted delivery of cisplatin-derived nanoprecursors via a biomimetic yeast microcapsule for tumor therapy by the oral route [J]. Theranostics. 2019;9(22):6568–86.
13. Wang J, Chen Y, Wang Q, Xu H, Wu C, Jiang Q, Wu G, Zhou H, Xiao Z, Chen Y, Zhang T, Lan Q. MEOX2-mediated regulation of cathepsin S promotes cell proliferation and motility in glioma [J]. Cell Death Dis. 2022;13(4):360.
14. Chen J, Li H, Zhang B, Xiong Z, Jin Z, Chen J, Zheng Y, Zhu X, Zhang S. ABI2-mediated MEOX2/KLF4-NANOG axis promotes liver cancer stem cell and drives tumour recurrence [J]. Liver Int. 2022;42(11):2562–76.
15. Liu XX, Bao QX, Li YM, Zhang YH. The promotion of cervical cancer progression by signal transducer and activator of transcription 1-induced upregulation of LncRNA MEOX2-AS1 as a competing endogenous RNA through miR-143-3p/VDAC1 pathway [J]. Bioengineered. 2021;12(1):3322–35.
16. Wang H, Tang Y, Yang X, Wang W, Han P, Zhao J, He S, Liu PA. Crucial angiogenesis-associated gene MEOX2 could be a promising biomarker candidate for breast cancer [J]. Front Oncol. 2022;12:759300.
17. Ferreira JA, Peixoto A, Neves M, Gaiteiro C, Reis CA, Assaraf YG, Santos LL. Mechanisms of cisplatin resistance and targeting of cancer stem cells: adding glycosylation to the equation [J]. Drug Resist Updat. 2016;24:34–54.
18. Maioru OV, Radoi VE, Coman MC, Hotinceanu IA, Dan A, Eftenoiu AE, Burtavel LM, Bohiltea LC, Severin EM. Developments in genetics: better management of ovarian cancer patients [J]. Int J Mol Sci. 2023;24(21):15987.
19. Yang D, He Y, Wu B, Deng Y, Wang N, Li M, Liu Y. Integrated bioinformatics analysis for the screening of hub genes and therapeutic drugs in ovarian cancer [J]. J Ovarian Res. 2020;13(1):10.
20. Guo N, Zhang J. Interleukin-17 promotes the development of ovarian cancer through upregulation of MTA1 expression [J]. Am J Cancer Res. 2022;12(12):5646–56.
21. Kuen DS, Kim BS, Chung Y. IL-17-producing cells in tumor immunity: friends or foes? [J]. Immune Netw. 2020;20(1):e6.
22. Rodriguez C, Araujo Furlan CL, Tosello Boari J, Bossio SN, Boccardo S, Fozzatti L, Canale FP, Beccaria CG, Nunez NG, Ceschin DG, Piaggio E, Gruppi A, Montes CL, Acosta Rodriguez, EV. Interleukin-17 signaling influences CD8(+) T cell immunity and tumor progression according to the IL-17 receptor subunit expression pattern in cancer cells [J]. Oncoimmunology. 2023;12(1):2261326.
23. Kryczek I, Banerjee M, Cheng P, Vatan L, Szeliga W, Wei S, Huang E, Finlayson E, Simeone D, Welling TH, Chang A, Coukos G, Liu R, Zou W. Phenotype, distribution, generation, and functional and clinical relevance of Th17 cells in the human tumor environments [J]. Blood. 2009;114(6):1141–9.
24. Rei M, Goncalves-Sousa N, Lanca T, Thompson RG, Mensurado S, Balkwill FR, Kulbe H, Pennington DJ, Silva-Santos B, Murine CD, -.) Vgamma6(+) gammadelta T cells producing IL-17A promote ovarian cancer growth via mobilization of protumor small peritoneal macrophages [J]. Proc Natl Acad Sci U S A. 2014;111(34):E3562–70.
25. Hu YY, Zhong RH, Guo XJ, Li GT, Zhou JY, Yang WJ, Ren BT, Zhu Y. Jinfeng pills ameliorate premature ovarian insufficiency induced by cyclophosphamide in rats and correlate to modulating IL-17A/IL-6 axis and MEK/ERK signals [J]. J Ethnopharmacol. 2023;307:116242.
26. Gorski DH, Leal AJ. Inhibition of endothelial cell activation by the homeobox gene Gax [J]. J Surg Res. 2003;111(1):91–9.
27. Chen Y, Banda M, Speyer CL, Smith JS, Rabson AB, Gorski DH. Regulation of the expression and activity of the antiangiogenic homeobox gene GAX/MEOX2 by ZEB2 and microRNA-221 [J]. Mol Cell Biol. 2010;30(15):3902–13.
28. Patel S, Leal AD, Gorski DH. The homeobox gene Gax inhibits angiogenesis through inhibition of nuclear factor-kappaB-dependent endothelial cell gene expression [J]. Cancer Res. 2005;65(4):1414–24.
29. Sarkar S, Rajput S, Tripathi AK, Mandal M. Targeted therapy against EGFR and VEGFR using ZD6474 enhances the therapeutic potential of UV-B phototherapy in breast cancer cells [J]. Mol Cancer. 2013;12(1):122.
30. Lim D, Do Y, Kwon BS, Chang W, Lee MS, Kim J, Cho JG. Angiogenesis and vasculogenic mimicry as therapeutic targets in ovarian cancer [J]. BMB Rep. 2020;53(6):291–8.
31. Wasik A, Ratajczak-Wielgomas K, Badzinski A, Dziegiel P, Podhorska-Okolow M. The role of Periostin in angiogenesis and lymphangiogenesis in tumors [J]. Cancers (Basel). 2022;14(17):4225.
32. Feng S, Xu Y, Dai Z, Yin H, Zhang K, Shen Y. Integrative Analysis From Multicenter Studies Identifies a WGCNA-Derived Cancer-Associated Fibroblast Signature for Ovarian Cancer [J]. Front Immunol, 2022, 13:951582.
33. Ding YL, Sun SF, Zhao GL. COL5A2 as a potential clinical biomarker for gastric cancer and renal metastasis [J]. Med (Baltim). 2021;100(7):e24561.
34. Ghosh S, Albitar L, LeBaron R, Welch WR, Samimi G, Birrer MJ, Berkowitz RS, Mok SC. Up-regulation of stromal versican expression in advanced stage serous ovarian cancer [J]. Gynecol Oncol. 2010;119(1):114–20.
35. Galluzzi L, Senovilla L, Vitale I, Michels J, Martins I, Kepp O, Castedo M, Kroemer G. Molecular mechanisms of cisplatin resistance [J]. Oncogene. 2012;31(15):1869–83.
36. Muggia F, Safra T. BRCAness' and its implications for platinum action in gynecologic cancer [J]. Anticancer Res. 2014;34(2):551–6.
37. Zhou Y, Nakajima R, Shirasawa M, Fikriyanti M, Zhao L, Iwanaga R, Bradford AP, Kurayoshi K, Araki K, Ohtani K. Expanding roles of the E2F-RB-p53 pathway in tumor suppression [J]. Biology (Basel). 2023;12(12):1511.
38. Iglesias-Ara A, Westendorp B, Editorial. The role of E2F transcription factors in cancer [J]. Front Oncol. 2023;13:1355610.
39. Sun Y, Cheng Z, Liu S. MCM2 in human cancer: functions, mechanisms, and clinical significance [J]. Mol Med. 2022;28(1):128.
40. Yang R, Zhang H, Chen Z, Zhang T, Wei P, Liang H, He Y, Zheng C, Wang X, Zhang Y. Drug resistance–related gene targets and molecular mechanisms in the A2780/Taxol–resistant epithelial ovarian cancer cell line [J]. Oncol Lett. 2024;27(5):232.

Publisher's note